



Europäisches  
Patentamt

European  
Patent Office

Office européen  
des brevets

#6  
N 17 514 us



Bescheinigung

Certificate

Attestation

Die angehefteten Unterla-  
gen stimmen mit der  
ursprünglich eingereichten  
Fassung der auf dem näch-  
sten Blatt bezeichneten  
europäischen Patentanmel-  
dung überein.

The attached documents  
are exact copies of the  
European patent application  
described on the following  
page, as originally filed.

Les documents fixés à  
cette attestation sont  
conformes à la version  
initialement déposée de  
la demande de brevet  
européen spécifiée à la  
page suivante.

Patentanmeldung Nr.    Patent application No.    Demande de brevet n°  
99202026.3

BEST AVAILABLE COPY

Der Präsident des Europäischen Patentamts;  
Im Auftrag

For the President of the European Patent Office

Le Président de l'Office européen des brevets  
p.o.

I.L.C. HATTEN-HECKMAN

DEN HAAG, DEN  
THE HAGUE,    18/01/00  
LA HAYE, LE

**THIS PAGE BLANK (USPTO)**



Europäisches  
Patentamt

European  
Patent Office

Office européen  
des brevets

**Blatt 2 der Bescheinigung**  
**Sheet 2 of the certificate**  
**Page 2 de l'attestation**

Anmeldung Nr.:  
Application no.:  
Demande n°: 99202026.3

Anmeldetag:  
Date of filing: 24/06/99  
Date de dépôt:

Anmelder:  
Applicant(s):  
Demandeur(s):  
Koninklijke Philips Electronics N.V.  
5621 BA Eindhoven  
NETHERLANDS

Bezeichnung der Erfindung:  
Title of the invention:  
Titre de l'invention:

Multiple input frequency domain adaptive filter ; acoustic echo and noise cancellation

In Anspruch genommene Priorität(en) / Priority(ies) claimed / Priorité(s) revendiquée(s)

Staat:  
State:  
Pays:

Tag:  
Date:  
Date:

Aktenzeichen:  
File no.  
Numéro de dépôt:

Internationale Patentklassifikation:  
International Patent classification:  
Classification internationale des brevets:

/

Am Anmeldetag benannte Vertragsstaaten:  
Contracting states designated at date of filing: AT/BE/CH/CY/DE/DK/ES/FI/FR/GB/GR/IE/IT/LI/LU/MC/NL/PT/SE  
Etats contractants désignés lors du dépôt:

Bemerkungen:  
Remarks:  
Remarques:

**THIS PAGE BLANK (USPTO)**

# Multiple Input Frequency Domain Adaptive Filter: Acoustic Echo and Noise Cancellation

G.P.M. Egelmeers

April 2, 1998

## 1 Introduction

### 1.1 Problem Description

Recent developments in audio and video systems require the use of multiple channel processing and reproduction with acoustic echo cancellers (AEC) and noise cancellers. In mini-group video conferencing systems multiple channel transmission leads to a better "localization" of the diverse people in the rooms. This enhances the intelligibility and naturalness of the speech. Stereo echo cancellation is needed in voice controlled stereo audio en video equipment. A multiple channel AEC can in general not be created by simple combination of multiple single AEC's. For two channel (stereo) AEC's this problem is well known and gets much attention in literature [11].

When the number of input signals in a multiple input acoustic echo canceller is larger then the number of independent signal (and noise) sources in a multiple input acoustic echo canceller there is no longer a unique solution for the adaptive filters. This is the so called "non-uniqueness" problem. In practice however, the number of independent sources is always larger than the number of microphones due to noise and other disturbances<sup>1</sup>. When however the power is not equally distributed over the independent sources, the problem might get badly conditioned, which is the main reason for the decrease in performance in the multiple input adaptive filters. In literature methods have been proposed to increase the performance by using Recursive Least Squares (RLS)-like algorithms (that have a huge computational complexity, even the most efficient implementations) and by adding non-linearities to the input signals (which might lead to audible artefacts in the output signal(s)).

Similar problems arise in the multiple channel noise cancellation where noise that is picked up by a microphone is reduced using extra microphone signals as noise reference signal [7, 8]. The reference signals are filtered and subtracted from the (delayed) primary microphone signal.

<sup>1</sup> "Non-uniqueness" is the name used in literature to describe the problem for the stereo acoustic echo canceller. When the input signals of a multiple input filter are filtered results of the same (single) source, there is no unique solution for the adaptive filter [11]. In practice this name "non-uniqueness" is not correct. As the 'alternative' solution in the stereo echo canceller case contains the product of a transfer function of a room and the inverse of another transfer function in the same room, it will in practice never be finite, meaning that there is in fact a unique solution. The presence of only a very small amount of noise (on for example the microphones) or the presence of at least as many sources as input signals to the multiple channel adaptive filter are other reasons why the "non-uniqueness" problem is in fact a problem of bad conditioning, see also [15].

Here we will present a multiple input frequency domain adaptive filter that makes use of the transformed inverse auto- and cross-correlation matrices to improve the performance of the adaptive filters without a huge increase in computational complexity.

## 1.2 Notation

Signals are denoted by lower case characters, constants by upper case. Underlining is used for vectors, lower case for time domain, and upper case for frequency domain. Matrices are denoted by caligraphic upper case, like  $\mathcal{X}$ , or bold face upper case, like  $\mathbf{I}$ . The dimension is put in superscript (e.g. the  $B \times Q$  matrix  $\mathcal{X}$  is given by  $\mathcal{X}^{B,Q}$ , for a square matrix the second dimension is omitted). Diagonal matrix are denoted by a double underline, like  $\underline{\underline{P}}$ , with its diagonal denoted as  $\underline{\underline{P}} = \text{diag}\{\underline{\underline{P}}\}$ . A subscript  $i$ , like  $\underline{w}_i$ , denotes the  $i$ 'th version. The  $\kappa$ 'th element of  $\underline{w}$  is given by  $(\underline{w})_\kappa$ . Finally, appending  $[k]$  denotes the time index,  $(\cdot)^T$  denotes the transpose,  $(\cdot)^*$  the complex conjugate and  $(\cdot)^H$  the Hermitain transpose (complex conjugate transpose).

## 2 Multiple Input Adaptive FIR Filter

### 2.1 Adaptive Filter Structure

A general multiple input adaptive FIR filter, depicted in figure 1, uses the  $S$  signals  $x_0[k]$  until  $x_{S-1}[k]$  to remove unwanted components related to these signals in the signal  $e_p[k]$ . The signals  $x_0[k]$  until  $x_{S-1}[k]$  are input to  $S$  FIR filters  $W_0$  until  $W_{S-1}$ , with outputs  $e_0[k]$  until  $e_{S-1}[k]$ . The goal of the update algorithm is to adapt the coefficients of the FIR filters in such a way that the correlation between  $e_p[k]$  and the input signals  $x_0[k]$  until  $x_{S-1}[k]$  is removed. For  $S > a \geq 0$  the FIR filter  $W_a$  performs the convolution of

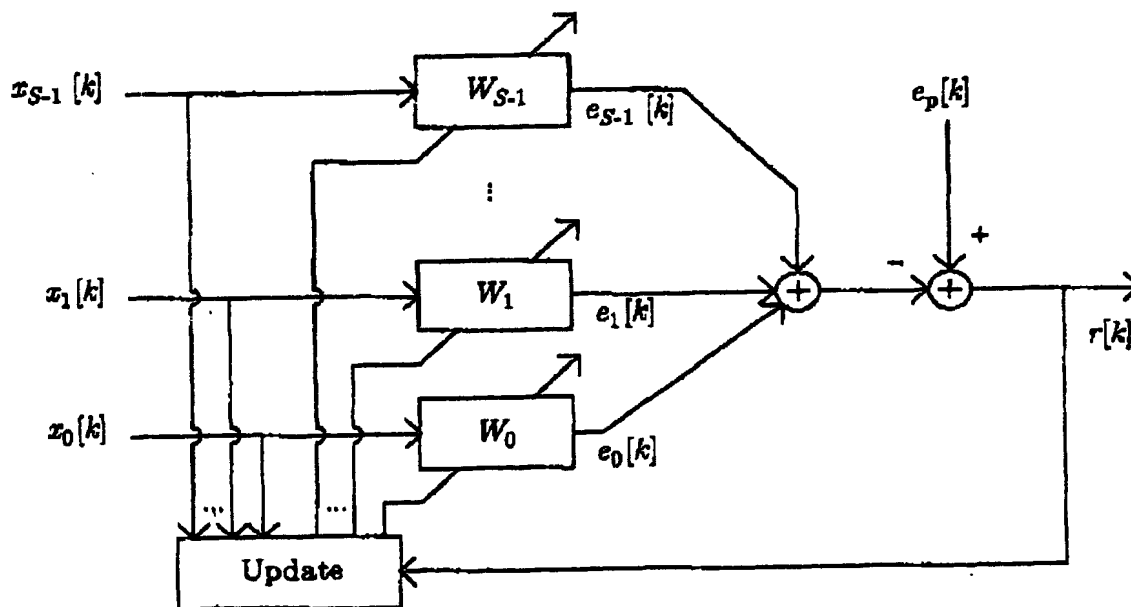


Figure 1: Multiple input adaptive FIR filter.

the signal  $x_a[k]$  and the coefficients  $w_{a,0} \dots w_{a,N-1}$  of that filter. The output signal  $e_a[k]$

of such a filter can be described as follows

$$\begin{aligned} e_a[k] &= \sum_{i=0}^{N-1} x_a[k-i] \cdot w_{a,i} \\ &= (\underline{x}_a^N[k])^t \cdot \underline{w}_a^N \end{aligned} \quad (1)$$

with for  $S > a \geq 0$

$$\underline{x}_a^N[k] = \begin{pmatrix} x_a[k-N+1] \\ \vdots \\ x_a[k-1] \\ x_a[k] \end{pmatrix} \quad (2)$$

$$\underline{w}_a^N = \begin{pmatrix} w_{a,N-1} \\ \vdots \\ w_{a,1} \\ w_{a,0} \end{pmatrix} \quad (3)$$

The output of the multiple input adaptive filter is given by

$$r[k] = e_p[k] - \sum_{a=0}^{S-1} e_a[k]. \quad (4)$$

These filter parts of the separate (adaptive) filters  $W_0$  until  $W_{S-1}$  can be implemented efficiently in frequency domain with help of partitioning, block processing and FFTs as described in [1, 2, 3, 6, 10].

For the update of the filter coefficients one can use  $S$  separate update algorithms. To improve convergence behaviour the input signals can be decorrelated separately in the time domain by using RLS like algorithms, leading to a huge computational complexity. Complexity reduction can be obtained by implementation in the frequency domain, with (Decoupled or Non-Uniform) Partitioned Block Frequency Domain Adaptive Filters (D or NU)-P3FDAF ([5, 6, 10, 12]). When there is correlation between the input signals of the filters this might however still lead to very bad convergence behaviour, see also [15], appendix C.

## 2.2 Multiple Input FDAF

We propose to use a partitioned algorithm in the frequency domain that reduces the effect of the crosscorrelation between the input signals on the algorithm's convergence behaviour. To reduce complexity we will use block processing with block length  $A$  to compute the sum of  $A$  consecutive updates with each iteration. We partition for  $S > a \geq 0$  the coefficient vectors  $\underline{w}_a^N[lA]$  into  $g_a$  parts of length  $Z$  with<sup>2</sup>  $g_a = \lceil N/Z \rceil$  such that for  $S > j \geq 0$

$$\underline{w}_j^N[lA] = \begin{pmatrix} \underline{w}_{j,g_a-1}^Z[lA] \\ \vdots \\ \underline{w}_{j,1}^Z[lA] \\ \underline{w}_{j,0}^Z[lA] \end{pmatrix} \quad (5)$$

<sup>2</sup>When  $N/Z$  is not an integer, all  $\underline{w}_a^N$  are extended to a length  $\lceil N/Z \rceil \cdot Z = g_a \cdot Z$  vector by appending  $\lceil N/Z \rceil \cdot Z - N$  coefficients that are kept zero.

25.214

with for  $S > j \geq 0$  and  $g_u > i \geq 0$

$$\underline{w}_{j,i}^Z[lA] = \begin{pmatrix} w_{j,iZ+Z-1}[lA] \\ \vdots \\ w_{j,iZ+1}[lA] \\ w_{j,iZ}[lA] \end{pmatrix}. \quad (6)$$

As we will use a Fourier transform length  $L$ , with  $L \geq Z + A - 1$ , we define the input signal Fourier transforms for  $S > a \geq 0$  as

$$\begin{aligned} \underline{X}_a^L[lA] &= \mathcal{F}^L \cdot \underline{x}_a^L[lA] \\ &= \mathcal{F}^L \cdot \begin{pmatrix} x_a[lA - L + 1] \\ \vdots \\ x_a[lA - 1] \\ x_a[lA] \end{pmatrix}. \end{aligned} \quad (7)$$

The diagonal matrices  $\underline{X}_a^L[lA]$  contain the vector  $\underline{X}_a^L[lA]$  as main diagonal, so for  $S > a \geq 0$

$$\underline{X}_a^L[lA] = \text{diag}\{\underline{X}_a^L[lA]\}. \quad (8)$$

As we use an overlap-save method to compute the correlation involved in the adaptation process in the frequency domain, the frequency domain transform of the residual signal vector equals

$$\underline{R}^L[lA] = \mathcal{F}^L \cdot \begin{pmatrix} 0^{L-A} \\ \underline{r}^A[lA] \end{pmatrix}. \quad (9)$$

The set of update equations for the filter coefficients in the MFDAF algorithm can now be defined for  $g_u > i \geq 0$  by (for a full derivation see [15])

$$\begin{pmatrix} \underline{w}_{S-1,i}^Z[(l+1)A] \\ \vdots \\ \underline{w}_{1,i}^Z[(l+1)A] \\ \underline{w}_{0,i}^Z[(l+1)A] \end{pmatrix} = \begin{pmatrix} \underline{w}_{S-1,i}^Z[lA] \\ \vdots \\ \underline{w}_{1,i}^Z[lA] \\ \underline{w}_{0,i}^Z[lA] \end{pmatrix} + \mathcal{G}^{S,Z,S,L} \cdot \begin{pmatrix} (\underline{Y}_{S-1}^L[lA - iZ])^* \\ \vdots \\ (\underline{Y}_1^L[lA - iZ])^* \\ (\underline{Y}_0^L[lA - iZ])^* \end{pmatrix} \cdot \underline{R}^L[lA] \quad (10)$$

with

$$\begin{pmatrix} (\underline{Y}_{S-1}^L[lA])^* \\ \vdots \\ (\underline{Y}_1^L[lA])^* \\ (\underline{Y}_0^L[lA])^* \end{pmatrix} = 2\alpha(\underline{P}^{S,L}[lA])^{-1} \cdot \begin{pmatrix} (\underline{X}_{S-1}^L[lA])^* \\ \vdots \\ (\underline{X}_1^L[lA])^* \\ (\underline{X}_0^L[lA])^* \end{pmatrix}. \quad (11)$$

and the transformation matrix  $\mathcal{G}^{S,Z,S,L}$  is given by

$$\mathcal{G}^{S,Z,S,L} = \begin{pmatrix} \mathcal{G}^{Z,L} & 0^{Z,L} & \dots & 0^{Z,L} \\ 0^{Z,L} & \ddots & \ddots & \vdots \\ \vdots & \ddots & \ddots & 0^{Z,L} \\ 0^{Z,L} & \dots & 0^{Z,L} & \mathcal{G}^{Z,L} \end{pmatrix} \quad (12)$$



with

$$\mathbf{G}^{Z,L} = \begin{pmatrix} \mathbf{J}^Z & \mathbf{0}^{Z,L-Z} \end{pmatrix} \cdot (\mathcal{F}^L)^{-1}. \quad (13)$$

In order to be able to use a delayline for the diverse input signal transforms, we have to choose  $Z$  in such a way that  $Z/A$  is integer, because then for all  $S > i \geq 0$   $(\mathbf{Y}^L[iA - iZ])^* = (\mathbf{Y}^L[(1 - i\frac{Z}{A})A])^*$  (see subsection 4.2.4 of [10]).

The input channel's power matrix  $\mathbf{P}^{S,L}[iA]$  is defined by

$$\begin{aligned} \mathbf{P}^{S,L}[iA] &= \frac{1}{L} \mathcal{E} \{ (\mathbf{X}^{S,L,L}[iA])^* \cdot (\mathbf{X}^{S,L,L}[iA])^t \} \\ &= \frac{1}{L} \begin{pmatrix} \mathcal{E} \{ (\mathbf{X}_{S-1}^L[iA])^* \mathbf{X}_{S-1}^L[iA] \} & \cdots & \mathcal{E} \{ (\mathbf{X}_{S-1}^L[iA])^* \mathbf{X}_0^L[iA] \} \\ \vdots & \ddots & \vdots \\ \mathcal{E} \{ (\mathbf{X}_0^L[iA])^* \mathbf{X}_{S-1}^L[iA] \} & \cdots & \mathcal{E} \{ (\mathbf{X}_0^L[iA])^* \mathbf{X}_0^L[iA] \} \end{pmatrix} \end{aligned} \quad (14)$$

where

$$\mathbf{X}^{S,L,L}[iA] = \begin{pmatrix} \mathbf{X}_{S-1}^L[iA] \\ \vdots \\ \mathbf{X}_1^L[iA] \\ \mathbf{X}_0^L[iA] \end{pmatrix} \quad (15)$$

The expectation operator  $\mathcal{E}\{\}$  of equation (14) has to be replaced by an estimation routine, which is the subject of section 2.3. As we need the inverse of  $\mathbf{P}^{S,L}[iA]$  a lot of divisions are required (in an algorithm to compute the inverse of this sparse matrix). We can reduce the number of operations by using a direct inverse matrix estimation algorithm, as is discussed in subsection 2.4. Note that the inverse of  $\mathbf{P}^{S,L}[iA]$  is also a sparse matrix with the same structure and we define

$$2\alpha(\mathbf{P}^{S,L}[iA])^{-1} = \begin{pmatrix} \mathbf{T}_{S-1,S-1}^L[iA] & \cdots & \mathbf{T}_{S-1,1}^L[iA] & \mathbf{T}_0^L[iA] \\ \vdots & \ddots & \vdots & \vdots \\ \mathbf{T}_{1,S-1}^L[iA] & \cdots & \mathbf{T}_{1,1}^L[iA] & \mathbf{T}_{1,0}^L[iA] \\ \mathbf{T}_{0,S-1}^L[iA] & \cdots & \mathbf{T}_{0,1}^L[iA] & \mathbf{T}_{0,0}^L[iA] \end{pmatrix} \quad (16)$$

where for  $0 \leq i < S$  and  $0 \leq j < S$

$$\mathbf{T}_{i,j}^L[iA] = \text{diag}\{\mathbf{T}_{i,j}^L[iA]\}. \quad (17)$$

In figures 2 and 3 the algorithm is depicted.

## 2.3 Power Estimation

### 2.3.1 Estimation of $2\alpha(\mathbf{P})^{-1}$

Estimation of  $2\alpha(\mathbf{P})^{-1}$  can be done by estimating  $\frac{\mathbf{P}}{2\alpha}$  and inverting the resulting matrix. The special structure of this matrix (and its inverse) implies that we need  $\frac{L}{2} - 1$  inversions of complex  $S \times S$  matrices and two inversions of real  $S \times S$  matrices. Because of estimation errors we need to limit the eigenvalues of  $\frac{\mathbf{P}}{2\alpha}$ , and we obtain from [15] the following estimation routine

$$\begin{aligned} \mathbf{P}_{\alpha, \text{lim}}^{S,L}[iA] &= (1 - \gamma) \cdot \mathbf{P}_{\alpha, \text{lim}}^{S,L}[(1 - 1)A] \\ &\quad + \gamma \cdot \left( \frac{1}{2\alpha L} \cdot (\mathbf{X}^{S,L,L}[iA])^* \cdot (\mathbf{X}^{S,L,L}[iA])^t + \frac{P_{\min}}{2\alpha} \cdot \mathbf{I}^{S,L} \right), \end{aligned} \quad (18)$$

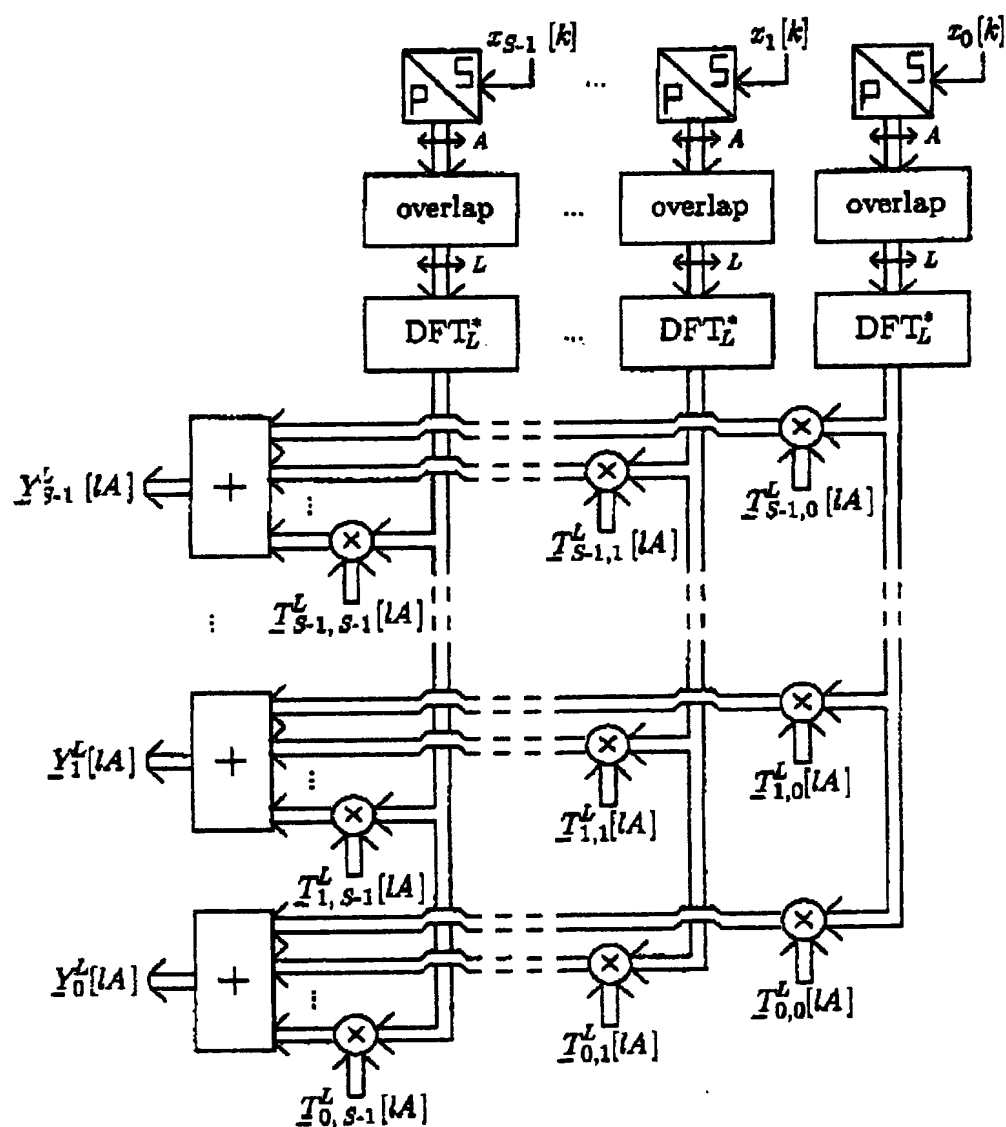


Figure 2: Calculate  $\underline{Y}$  in MPBFDAF.

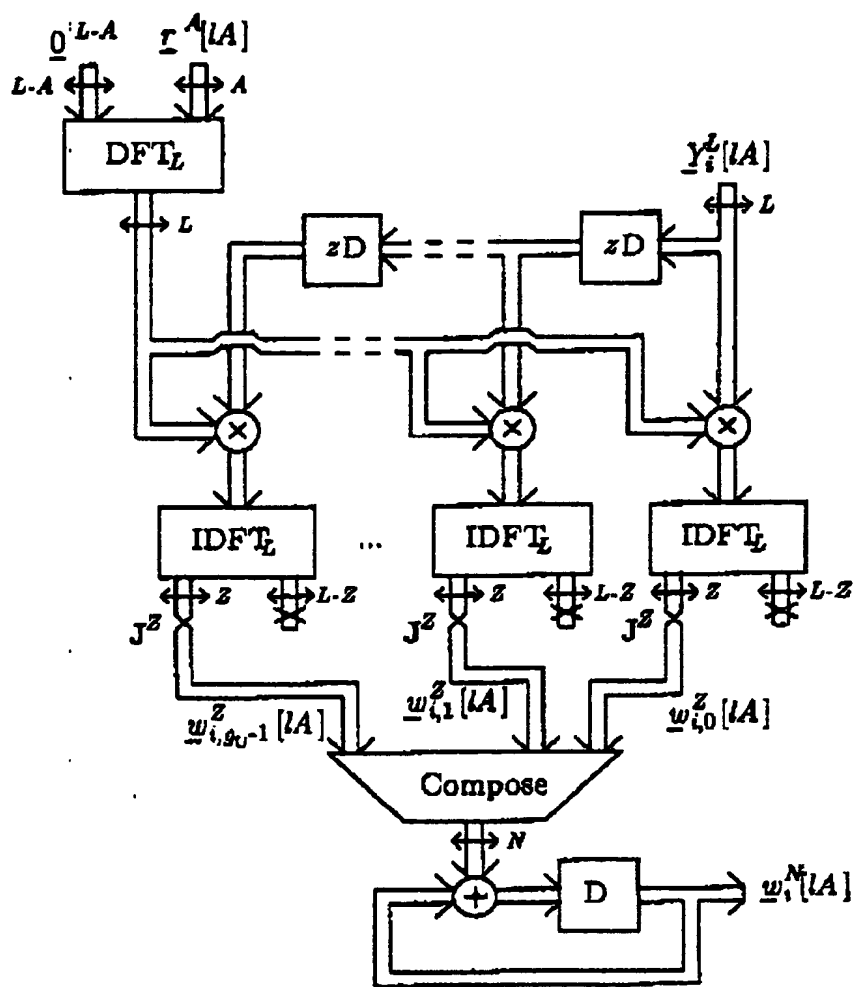


Figure 3: Calculate  $w_i^N[lA]$  in MPBFDAF.

where  $P_{\min}$  is the eigenvalueshift (and thus the minimum for the eigenvalues of  $P_{\alpha, \lim}^{S, L}[lA]$ ).  
 In appendix A the initialization for the estimation routine is described.

## 2.4 Estimation of Inverse

### 2.4.1 Plain Borders

To avoid the matrix inversions we can also use a direct estimate of the inverse power matrix. To guarantee stability we have to use an algorithm that keeps the eigenvalues positive. In [15], such an algorithm is derived and the results are summarized in table 1. In appendix A the initialization of the inverse power matrix is discussed.

#### Initialization

1.  $S_u = 2^{\lceil \log_2 S + 1 \rceil}$
2.  $U^1 = \sqrt{P_{\min} \cdot 2\alpha L}$   
 for  $i = 1$  to  $\log_2(S_u)$  do  
 begin  

$$U^{2^i} = \begin{pmatrix} U^{2^{i-1}} & U^{2^{i-1}} \\ U^{2^{i-1}} & -U^{2^{i-1}} \end{pmatrix}$$
  
 end

3. Initialize power matrix (see appendix A).

#### Iteration

1. 
$$X_{\lim}^{S, L, L}[lA] = \begin{pmatrix} \underline{X}_0^L[lA] \\ \underline{X}_1^L[lA] \\ \vdots \\ \underline{X}_{S-1}^L[lA] \end{pmatrix} + \begin{pmatrix} u_{S_u-S, l \bmod S_u} \cdot I^L \\ u_{S_u-S+1, l \bmod S_u} \cdot I^L \\ \vdots \\ u_{S_u-1, l \bmod S_u} \cdot I^L \end{pmatrix}$$
2. 
$$Q^{S, L, L}[lA] = \frac{1}{1-\gamma} \cdot (P_{\alpha, \lim}^{S, L}[(l-1)A])^{-1} \cdot (X_{\lim}^{S, L, L}[lA])^*$$
3. 
$$\underline{D}^L[lA] = \frac{2\alpha L}{\gamma} I^L + (X_{\lim}^{S, L, L}[lA])^* \cdot Q^{S, L, L}[lA]$$
4. Calculate  $(\underline{D}^L[lA])^{-1}$
5. 
$$(P_{\alpha, \lim}^{S, L}[lA])^{-1} = \frac{1}{1-\gamma} (P_{\alpha, \lim}^{S, L}[(l-1)A])^{-1} - Q^{S, L, L}[lA] \cdot (\underline{D}^L[lA])^{-1} \cdot (Q^{S, L, L}[lA])^h$$

Table 1: Direct inverse power update with limits.

### 2.4.2 Power Matrix Dimension Reduction

Partitioning of the coefficient vectors implies a reduction in the dimension of the power vector and an increase in both the adaptive filter update rate and the update rate of the power matrix estimate (assuming that the block length is in the same order as the

partition length)<sup>3</sup>. Due to the increased rate and the reduced dimension we can make a much more accurate estimate of the inverse power matrix. Besides that, the tracking of the non-stationarities in the input signal power is improved and, due to the increased rate in the update part, also the tracking of the non-stationarities in the unknown path, see also 2.5.4 and 4.4.3 in [10].

### 2.4.3 Decoupling Power Estimate

Partitioning of the coefficient vector increases the computational complexity. When the main cause of trouble is the tracking of the input signal power, we can reduce the dimension of the input signal power matrix and increase its update rate independent from the partition length of the coefficient vector. We then can obtain part of the advantages of partitioning with a much smaller increase in complexity, see subsection 6.4.2 in [10].

## 3 Computational Complexity

To obtain a rough estimate of the effect on the computational complexity of the proposed algorithm, we will compare our MFDFAF algorithm with using  $S$  separate DPBFDAF algorithms. We define  $G_*$  and  $G_+$  as the number of operations needed for a multiplication and an addition.  $G_P$  and  $G_{(P)-1}$  denote the number of operations needed for the estimation of  $P$ , indirect (subsection 2.3.1) or direct (subsection 2.4).  $F\{L\}$  denotes the number of operations needed for a length  $L$  real input FFT. The total number of real operations for the update part per block of  $A$  samples is summarized in table 2 (see [15]).

	Separate DPBFDAFs	Multiple Input BFDAF
1) FFTs	$((1 + g_*) \cdot S + 1) \cdot F\{L\}$	
$P^{-1}$ indirect [15], ss. 3.1.3	$S \cdot G_P\{1\} + G_{-1}\{1\}$	$G_P\{S\} + G_{-1}\{S\}$
$P^{-1}$ direct [15], ss. 3.2.4	$S \cdot G_{(P)-1}\{1\}$	$G_{(P)-1}\{S\}$
$P^{-1} \cdot X$	$L \cdot S \cdot G_*$	$L \cdot S \cdot ((2 \cdot S - 1) \cdot G_* + (S - 1) \cdot G_+)$
$(P^{-1} \cdot X) \cdot R$	$g_+ \cdot L \cdot S \cdot (2 \cdot G_* + G_+)$	
$W + W_\Delta$	$S \cdot N G_+$	

Table 2: Real operations per  $A$  samples for update algorithms.

When we compare the Multiple Input BFDAF to the separated channels case, we see that there is a difference in the number of elementwise multiplications and in the power update. The main computational load however, is caused by the computation of the FFTs, so this increase will only make a small relative difference (depending on  $S$ ). For example, when we use split-radix FFTs whose complexity is given in table 3, that  $G_+ = G_* = 1$  (see [10]) and that  $G_P = 5$ , and take  $N = 2048$ ,  $A = Z = 512$ ,  $L = 1024$ ,  $g_u = 4$  and

<sup>3</sup>The rate depends only on the block length, but this block length is strongly related to the partition length in order to keep the computational complexity as low as possible. We can of course also reduce the block length and thus increase the rate without partitioning. This however leads to a huge increase in computational complexity (see [10]).

$L$	$F_+ \text{ (in } G_+)$	$F_+ \text{ (in } G_+)$
2	0	2
4	0	6
8	2	20
16	12	58
32	42	154
64	122	392
128	328	950
256	822	2240
512	1984	5158
1024	4646	11680
2048	10656	26086
4096	24038	57632

Table 3: Operations for split-radix real input FFT.

the cases  $S = 2$  and  $S = 3$ , we get with help of table 2, the results of table 4. We can see that there is an increase of approximately 10 % per extra input channel of the multiple input BFDFAF compared to the separate DPBFDFAF's. As the update part takes approximately 50 % of the computational load in the BFDFAF case (the other half is needed for the actual filtering operation), the increase in computational complexity for the whole multiple channel adaptive filter is about 5 % per extra input channel. For  $S \geq 4$  the computational complexity of the direct inverse power estimate is much smaller then the computational complexity of the power estimate and matrix inversion method.

Operation	Separate DPBFDFAFs				Multiple Input BFDFAF			
	$S = 2$	$S = 3$	$S = 4$	$S = 8$	$S = 2$	$S = 3$	$S = 4$	$S = 8$
(I) FFTs	351	510	670	1307	351	510	670	1307
$P^{-1}$ (indirect)	30	45	60	120	50	146	904	6712
$P^{-1}$ (direct)	52	78	104	208	81	170	293	1125
$P^{-1} \cdot X$	4	6	8	16	16	42	80	352
$(P^{-1} \cdot X) \cdot R$	48	72	96	192	48	72	96	192
$u + u_{\Delta}$	8	12	16	32	8	12	16	32
Total (indirect)	441	645	850	1667	473	782	1766	8595
Total (direct)	463	678	894	1755	504	806	1155	3008
Optimum	441	645	850	1667	473	782	1155	3008
Increase for MFDAF					7 %	21 %	36 %	80 %

Table 4: Example real operations per sample for update algorithms.

## 4 Applications

### 4.1 Stereo Acoustic Echo Canceller

A full stereo communication requires four stereo AECs, two on the near end side and two on the far end side. In figure 4 one of those echo cancellers is depicted. Note that on each side we can combine the input signal delay-lines, the FFTs and the multiplication by the inverse power matrix of the two echo cancellers, which implies that the relative extra computational complexity for removing the crosscorrelation is even further reduced. The performance of the AECs is further improved by adding Dynamic Echo Suppressors

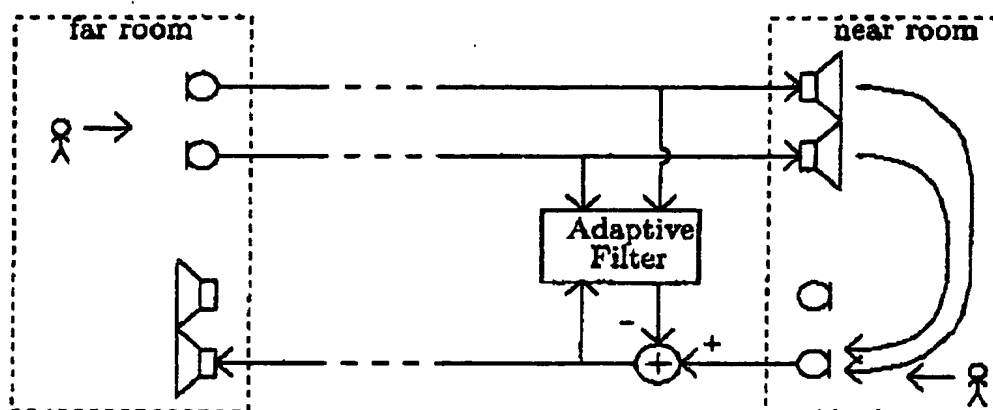


Figure 4: Isolated Adaptive Filter in Stereo Echo Cancellation.

(DES) and programmable filters, see [4, 13, 14], leading to the configuration in figure 5.

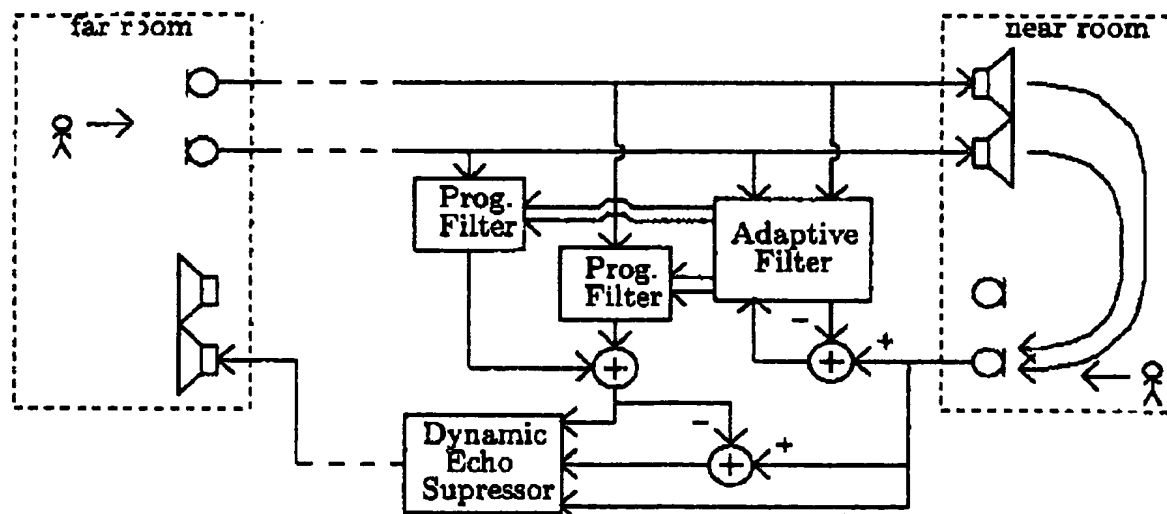


Figure 5: Isolated Adaptive Filter with Dynamic Echo Suppressor.

## 4.2 Multiple Input Adaptive Noise Canceller

A second application for the multiple input adaptive filter is the multiple input noise canceller. The first configuration is depicted in figure 6. The microphones are placed in a cross<sup>4</sup>. We use a selection mechanism to select the microphone where the desired signal (speaker) is located and use the other microphone signals ( $x_0[k]$  until  $x_2[k]$  (or, more general,  $x_{S-1}[k]$ )) to cancel the other signal sources.

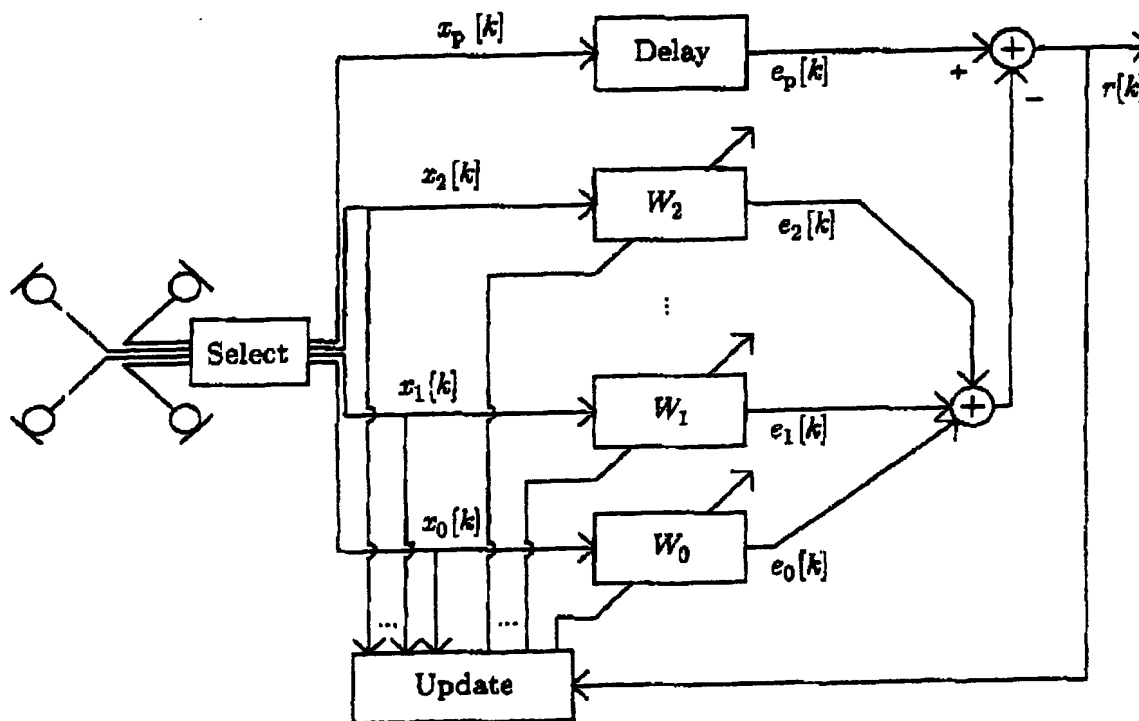


Figure 6: Adaptive Noise Canceller with a Cross Configuration.

A second configuration tries to select the desired signal from an array of microphones using a delay-sum beamformer, and creates noise (unwanted signals) references by subtraction, see figure 7. Also in the multiple input Noise Canceller we can apply Dynamic Echo Suppressors (which is in fact not suppressing an echo, but is similar to the DES in the AECs case) and programmable filters to improve performance (which is not depicted here). An extra problem is that the inputs of the filters may contain some elements of the desired signal ("signal leakage", because the delay-sum beamformer is not perfect and/or the directional microphones in the cross configuration are not ideal). When the desired signal is a speech signal, a speech detector can be used to improve the behaviour of the MFDAF. Another solution to suppress the influence of the signal leakage is given in [9].

<sup>4</sup>The number of microphones is of course not restricted to four.



25.214

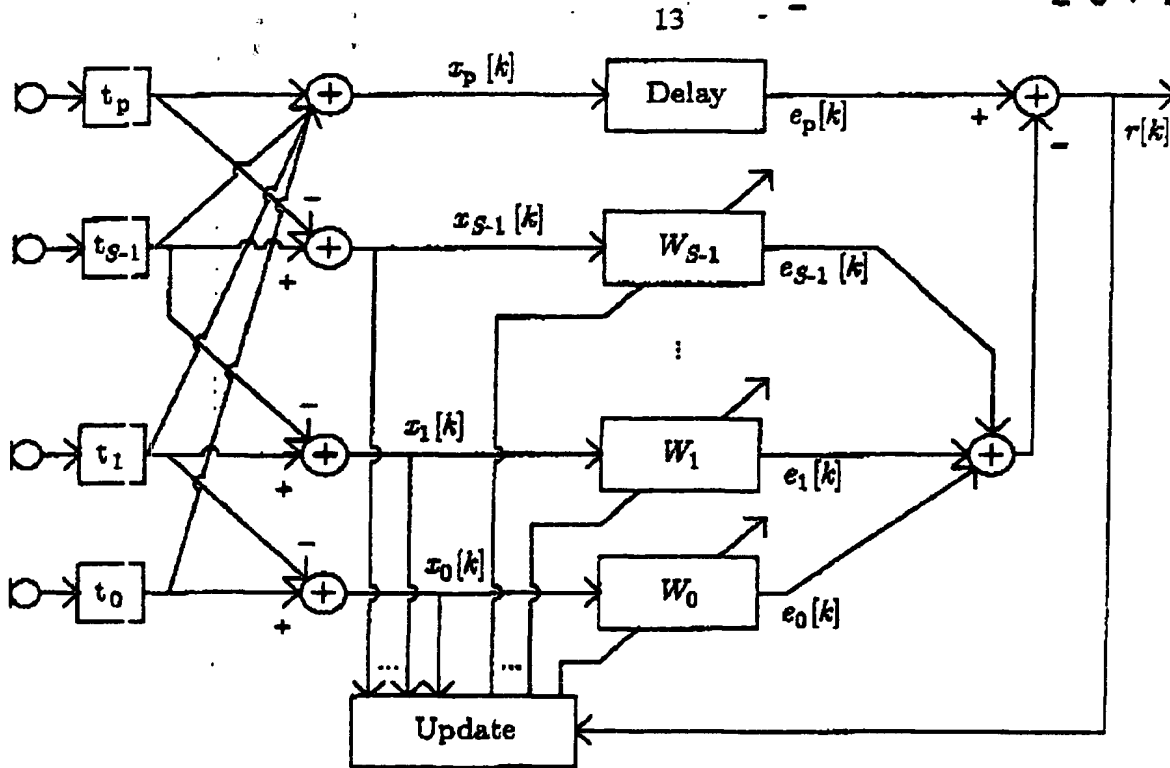


Figure 7: Adaptive Noise Canceller with a Linear Array.

## 5 Conclusions

A Multiple input Frequency Domain Adaptive Filter (MFDAF) algorithm is presented that uses partitioning and decorrelation techniques in the frequency domain to improve convergence behaviour, especially in highly correlated and/or non-stationary environment. The conditioning of the problem is greatly improved by using estimates of the transformed auto- and crosscorrelation matrices (see [15], appendix C). Efficient algorithms for the estimation of the inverse transformed auto- and crosscorrelation matrices are presented so using MFDAF does not lead to a huge increase in computational complexity compared to using multiple single input adaptive filters. The main applications are the stereo Acoustic Echo Canceller and the multiple input adaptive Noise Canceller.

## A Initialization of power matrix

### A.1 Estimation of P

Equation (18) that describes the power matrix update, was given by

$$\mathbf{P}_{\alpha, \text{lim}}^{S, L}[lA] = (1 - \gamma) \cdot \mathbf{P}_{\alpha, \text{lim}}^{S, L}[(l-1)A] + \gamma \cdot \left( \frac{1}{2\alpha L} \cdot (\mathbf{X}^{S, L, L}[lA])^* \cdot (\mathbf{X}^{S, L, L}[lA])^t + \frac{P_{\text{min}}}{2\alpha} \cdot \mathbf{I}^{S, L} \right). \quad (19)$$

From the above equation we see that (for  $i \geq l$ )  $(\mathbf{X}^{S, L, L}[(l-i)A])^* \cdot (\mathbf{X}^{S, L, L}[(l-i)A])^t$  is weighted by a factor  $(1 - \gamma)^i$  compared to  $(\mathbf{X}^{S, L, L}[lA])^* \cdot (\mathbf{X}^{S, L, L}[lA])^t$ . As we do not

have any a priori knowledge of the input signals, we cannot make an accurate guess for the initial power matrix  $P_{\sigma, \text{lim}}^{S, L}[-A]$ . When we assume that it equal the all zero matrix, the matrix  $P_{\sigma, \text{lim}}^{S, L}[IA]$  is a factor  $1 - (1 - \gamma)^{l+1}$  too small (in a stationary environment). We therefore propose to use  $P_{\sigma, \text{lim, init}}^{S, L}[IA]$ , with

$$P_{\alpha, \text{lim}, \text{init}}^{S, L}[IA] = \frac{1}{1 - (1 - \gamma)^{L+1}} \cdot P_{\alpha, \text{lim}}^{S, L}[IA]. \quad (20)$$

**This implies that**

$$\mathbf{P}_{\alpha, \text{lim, init}}^{S, L}[lA] = (1 - \gamma) \cdot \frac{1 - (1 - \gamma)^l}{1 - (1 - \gamma)^{l+1}} \cdot \mathbf{P}_{\alpha, \text{lim, init}}^{S, L}[(l - 1)A] \\ + \frac{\gamma}{1 - (1 - \gamma)^{l+1}} \cdot \left( \frac{1}{2\alpha L} \cdot (\mathbf{X}^{S, L, L}[lA])^* \cdot (\mathbf{X}^{S, L, L}[lA])^T + \frac{P_{\min}}{2\alpha} \cdot \mathbf{I}^{S, L} \right). \quad (21)$$

As this takes a few extra multiplications and divisions, we propose to do this until  $1 - (1 - \gamma)^{i+1}$  is close to 1 (e.g.  $> 0.95$ ), and then switch to the not corrected formula (with the corrected power matrix as first guess).

## A.2 Estimation of Inverse

For the direct inverse power matrix estimation we use in table 1

$$(\mathbf{P}_{\alpha, \text{lim}}^{S, L}[\mathbf{I}A])^{-1} = \frac{1}{1-\gamma} (\mathbf{P}_{\alpha, \text{lim}}^{S, L}[(l-1)A])^{-1} - \mathbf{Q}^{S, L, L}[\mathbf{I}A] \cdot (\mathbf{D}^L[\mathbf{I}A])^{-1} \cdot (\mathbf{Q}^{S, L, L}[\mathbf{I}A])^h \quad (22)$$

**with**

$$\mathbf{Q}^{S \cdot L, L}[IA] = \frac{1}{1-\gamma} \cdot (\mathbf{P}_{\alpha, \lim}^{S \cdot L}[(l-1)A])^{-1} \cdot (\mathbf{X}_{\lim}^{S \cdot L, L}[IA])^* \quad (23)$$

and

$$\underline{\underline{\mathbf{D}}}^L[A] = \frac{2\alpha L}{\gamma} \mathbf{I}^L + (\mathbf{X}_{\text{lim}}^{S \cdot L, L}[A])^t \cdot \mathbf{Q}^{S \cdot L, L}[A]. \quad (24)$$

Here we do not have the possibility of an initial guess with the zero matrix for  $(P_{\alpha, \lim}^S[-A])^{-1}$ , because then the algorithm would always yield a zero matrix as result. We therefore suggest to use a momentaneous estimate of the diagonal of  $P_{\alpha, \lim}^S[0]$ , so

$$(\mathbf{P}_{\alpha, \lim, i}^{S \cdot L})^{-1} [-A]^{-1} = \left( \frac{1}{2\alpha L} \begin{pmatrix} (\underline{\mathbf{X}}_0^L[0])^* \cdot \underline{\mathbf{X}}_0^L[0] & 0^L & \dots & 0^L \\ 0^L & \ddots & \ddots & \vdots \\ \vdots & \ddots & \ddots & 0^L \\ 0^L & \dots & 0^L & (\underline{\mathbf{X}}_{S-1}^L[0])^* \cdot \underline{\mathbf{X}}_{S-1}^L[0] \end{pmatrix} + \frac{P_{\min}}{2\alpha} \cdot \mathbf{I}^{S \cdot L} \right)^{-1} \quad (25)$$

which means that we have to calculate  $S \cdot L$  divisions. To get a fair weighting of the input vectors in the first iterations, also here we have to adjust the multiplication factors in the update algorithm. In the first iterations  $\gamma$  must be chosen larger to get a better

25.214

15.

estimate of the full power matrix, so we propose to use  $\gamma_{init} \cdot (1 - \gamma)^l$  instead of  $\gamma$  as long as  $\gamma_{init} \cdot (1 - \gamma)^l$  is larger than  $\gamma$ .<sup>5</sup>

$$(P_{\alpha,lim,init}^{S,L}[lA])^{-1} = \frac{1}{1 - \gamma_{init} \cdot (1 - \gamma)^l} \cdot (P_{\alpha,lim,init}^{S,L}[(l-1)A])^{-1} - Q^{S,L,L}[lA] \cdot (\underline{D}^L[lA])^{-1} \cdot (Q^{S,L,L}[lA])^h \quad (26)$$

with

$$Q^{S,L,L}[lA] = \frac{1}{1 - \gamma_{init} \cdot (1 - \gamma)^l} \cdot (P_{\alpha,lim}^{S,L}[(l-1)A])^{-1} \cdot (X_{lim}^{S,L,L}[lA])^* \quad (27)$$

and

$$\underline{D}^L[lA] = \frac{2\alpha L}{\gamma_{init} \cdot (1 - \gamma)^l} I^L + (X_{lim}^{S,L,L}[lA])^t \cdot Q^{S,L,L}[lA]. \quad (28)$$

## B Instabilities

The power matrix estimation and inversion algorithms do not give an absolute guarantee that the loop of the adaptive filter is stable. The estimation errors and approximations used to make the correlation matrices circulant may result in a temporarily feed back gain for one of the eigenmodii in the adaptive filter that is too large, especially when the input signal is highly non-stationary. To guarantee stable operation of the MFDAP algorithm (including programmable filters) we therefore need to check if such instabilities occur and reinitialize the power matrix (and filter coefficients) if necessary. The coefficients calculated by the adaptive filter are only transferred to the programmable filters (that calculate the actual output of the system), when this leads to a reduction in the power of the output signal (residual signal) (see [13]). Instability therefore means that the output generated by the adaptive filter explodes, while the actual output (generated by the programmable filters) does not do that.

We detect instabilities by comparing the mean squared value of the adaptive filter output by the mean squared value of the programmable filters output. When this ratio exceeds a certain threshold ( $\gg 1$ ) and there is relevant input<sup>6</sup> the adaptive filter is reset (the power matrix is reinitialized and the coefficients are put to zero).

<sup>5</sup>Note that  $\gamma_{init}$  cannot be 1, as we divide by  $1 - \gamma_{init}$  in the first iteration!

<sup>6</sup>This is checked by demanding that the ratio of the power of the adaptive filter output and the power of the signal that must be corrected exceeds the same threshold. When this happens, the signal to correct is much smaller than the signal it is corrected by, this certainly does not improve the result.

**CLAIMS:**

1. Stereo acoustic echo canceller comprising decorrelation means.
2. Adaptive noise canceller comprising decorrelation means.
- 5 3. Decorrelation means for use in a stereo acoustic echo canceller as claimed in claim 1
4. Decorrelation means for use in a adaptive noise canceller as claimed in claim 2.
- 10 5. Method of decorrelation of at least two signals.

**This Page is Inserted by IFW Indexing and Scanning  
Operations and is not part of the Official Record**

**BEST AVAILABLE IMAGES**

Defective images within this document are accurate representations of the original documents submitted by the applicant.

Defects in the images include but are not limited to the items checked:

- ☐ **BLACK BORDERS**
- ☐ **IMAGE CUT OFF AT TOP, BOTTOM OR SIDES**
- ☐ **FADED TEXT OR DRAWING**
- ☒ **BLURRED OR ILLEGIBLE TEXT OR DRAWING**
- ☐ **SKEWED/SLANTED IMAGES**
- ☐ **COLOR OR BLACK AND WHITE PHOTOGRAPHS**
- ☐ **GRAY SCALE DOCUMENTS**
- ☐ **LINES OR MARKS ON ORIGINAL DOCUMENT**
- ☐ **REFERENCE(S) OR EXHIBIT(S) SUBMITTED ARE POOR QUALITY**
- ☐ **OTHER:** \_\_\_\_\_

**IMAGES ARE BEST AVAILABLE COPY.**

**As rescanning these documents will not correct the image problems checked, please do not report these problems to the IFW Image Problem Mailbox.**

**THIS PAGE BLANK (USPTO)**